ACS OMEGA

http://pubs.acs.org/journal/acsodf

Article

UPLC-Q-TOF/MS-Based Serum Metabolomics Reveals the Anti-Ischemic Stroke Mechanism of Nuciferine in MCAO Rats

Lanlan Wu,[#] Chang Chen,[#] Yongbiao Li, Cong Guo, Yuqing Fan, Dingrong Yu, Tinglan Zhang, Binyu Wen,* Zhiyong Yan,* and An Liu*

Cite This: *ACS Omega* 2020, 5, 33433−33444

Read Online

ACCESS | Metrics & More | Article Recommendations | Supporting Information

ABSTRACT: Nuciferine is an aporphine alkaloid monomer that is extracted from the leaves of the lotus species *Nymphaea caerulea* and *Nelumbo nucifera* Gaertn. Nuciferine was reported to treat cerebrovascular diseases. However, the potential mechanism of the neuroprotective effects of nuciferine at the metabolomics level is still not unclear. The present research used neurological score, infarct volume, cerebral water content, and ultraperformance liquid chromatography to quadrupole time-of-flight mass spectrometry (UPLC-Q-TOF/MS)-based serum metabolomics to elucidate the anti-ischemic stroke effect and mechanisms of nuciferine. The results showed that nuciferine significantly improved neurological deficit scores and ameliorated cerebral edema and infarction. Multivariate data analysis methods were used to examine the differences in serum endogenous metabolism between groups, and the biomarkers of nuciferine on ischemic stroke were identified. Approximately 19 metabolites and 7 metabolic pathways associated with nuciferine on treatment of stroke were found, which indicated that nuciferine exerted a positive therapeutic action on cerebral ischemic by regulating metabolism. These results provided some data support for the study of anti-stroke effect of nuciferine from the perspective of metabolomics.

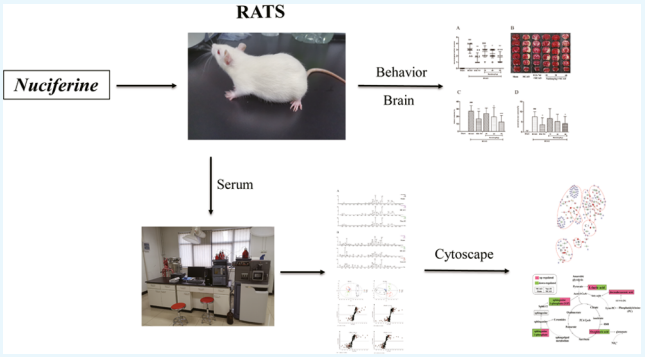

INTRODUCTION

Globally, stroke is one of the most serious diseases threatening human life and health, and approximately 87% of stroke cases belong to the ischemic category.[1,2] Among different stroke types, ischemic stroke has the highest rates of morbidity, disability, and mortality.[3] The etiology of ischemic disease is associated with internal carotid artery occlusion and stenosis.[4] Increasing evidence shows that excitatory amino acid toxicity, energy failure, metabolic disorders, and inflammation are the main causes of stroke.[5] Stroke treatment options and the therapeutic time window are extremely limited in clinical practice.[6] Therefore, only a few patients who are in the right place within the right time frame can be treated after the onset of symptoms. Moreover, a series of severe side effects accompany treatment measures, such as postperfusion lesions and hemorrhage, which hinder the effective treatment of patients and may aggravate the disease.[7] Therefore, better treatment and fewer adverse reactions are urgently needed to overcome the clinical therapeutic limitations. Traditional Chinese medicine (TCM) has been used to treat ischemic stroke for thousands of years.[8−10] Some studies confirmed that the safety, effectiveness, and multitarget characteristics of TCM have significant advantages in the treatment of ischemic stroke.[11−13]

Lotus is a famous Chinese medicine with high nutritional and medicinal value, and it was initially recorded in the Chinese Pharmacopoeia. Previous studies found many bioactive alkaloids in lotus leaf, primarily *N*-nornuciferine, neferine, and nuciferine. Nuciferine ((*R*)-1, 2-dimethoxyaporphine; Nuci) is a major natural bioactive alkaloid containing an aromatic ring and was widely used in ancient China and India. Nuciferine is used to improve hepatic lipid metabolism,[14] and it exhibits anti-inflammatory,[15] antimicrobial,[16] antioxidant,[17] and antifibrosis[18] activity, as well as other cardiovascular-protective actions.[19] Nuciferine enters the brain through the blood−brain barrier.[20] However, an overview of the research both domestically and abroad revealed few studies on the anti-stroke properties and the mechanism of action of nuciferine, and our understanding of endogenous substance-related metabolism in the state of cerebral ischemia is also poor. Therefore, we focused on the monomer component of effective TCM, nuciferine, to clarify its anti-ischemic stroke mechanism.

Received: November 4, 2020
Accepted: December 3, 2020
Published: December 15, 2020

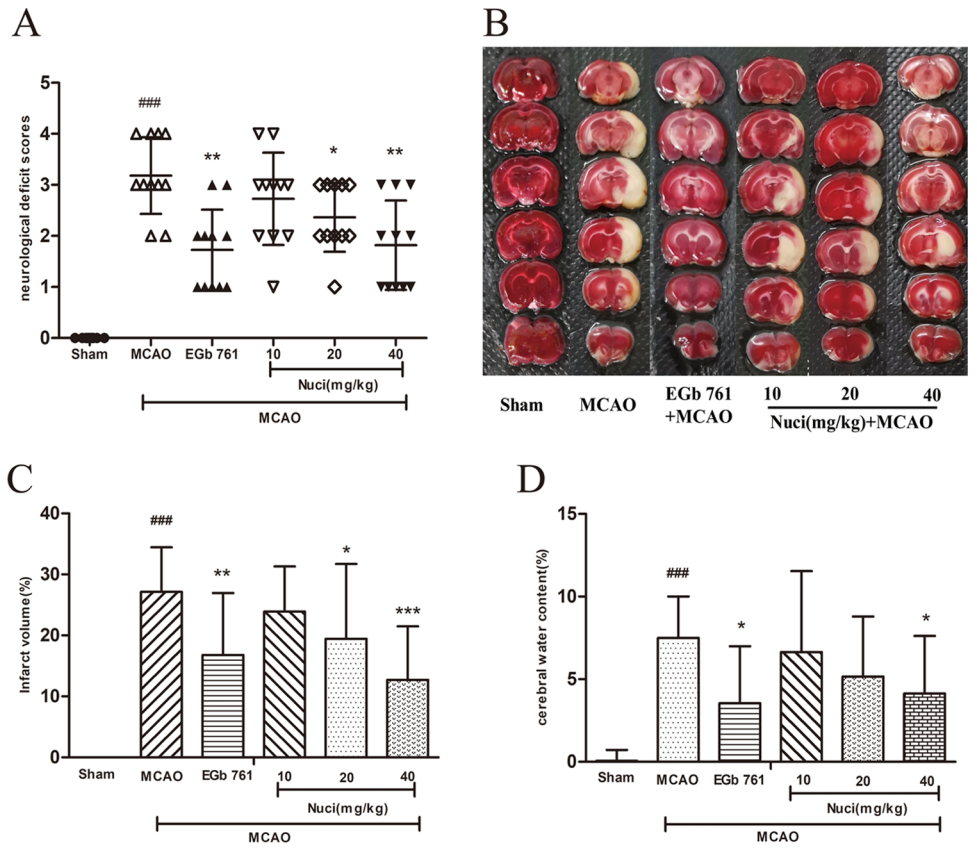

Figure 1. Anti-ischemic cerebral effects of different doses of nuciferine in MCAO rats. Results of neurological deficit scores (A), infarct volume (B, C), and cerebral water content (D) (n = 11 per group). All groups were administered intragastrically 30 min prior to MCAO. Neurological deficit scores were dramatically higher than the sham group after MCAO ($P < 0.001$). However, pretreatment with EGb 761 and a high dose of nuciferine significantly reduced the scores ($P < 0.01$). (B) TTC staining photograph. Red, healthy tissue; white, infarcted tissue. (C, D) Quantitative analyses of infarct volume and brain water content, respectively. After administration of Nuci-H, infarct volume, and cerebral water content decreased ($P < 0.001$ or $P < 0.05$). Data are expressed as mean ± SD. #$P < 0.05$, ##$P < 0.01$, ###$P < 0.001$ vs sham group; *$P < 0.05$, **$P < 0.01$, ***$P < 0.001$ vs MCAO group.

Metabolomics is a universally applicable method for the comprehensive metabolic profiling of biological samples that reflects the overall functional state of the body and monitors disease progression according to dynamic changes in metabolites.[21] Ultraperformance liquid chromatography to quadrupole time-of-flight mass spectrometry (UPLC-Q-TOF/MS) is a premier tool for investigating the curative effects of Chinese medicine, and it is used to measure small molecules in biological samples, including serum, urine, and feces, and to describe metabolic abnormalities during pathological processes.[22] Therefore, UPLC-Q-TOF/MS-based metabolomics was used to screen and identify biomarkers and metabolic pathways related to ischemic stroke in this study, and the mechanism of the anti-ischemic action of nuciferine was preliminarily studied at the level of small molecular metabolites, which provide supporting data for further study.

In the present study, the metabolic profiles of serum samples from nuciferine-treated and untreated rats were analyzed to screen potential biomarkers of brain damage and explore neuroprotective potential of nuciferine. Then, the metabolic pathways and characteristic metabolites associated with ischemic stroke were explored by combining the pharmacodynamic index and metabolic markers to clarify anti-stroke mechanisms of action of nuciferine.

RESULTS

Effects of Nuciferine on Neurological Deficit Scores, Infarct Volume, and Cerebral Water Content after MCAO in Rats. To evaluate the protective effect of nuciferine on cerebral ischemia, the MCAO model was established, and data from behavioral and pharmacodynamics support its success. The present study statistically analyzed the neurological function scores of rats (Figure 1A). After the MCAO surgical intervention, the scores of the MCAO group significantly increased compared to those in the sham group ($P < 0.001$), which verified the stability of the MCAO model. The scores of rats decreased in all administration groups, and the scores of the Nuci-H, Nuci-M, and EGb 761 groups significantly decreased ($P < 0.01$, $P < 0.05$).

MCAO induced brain injury, which primarily manifested as cerebral infarct (Figure 1B,C) and edema (Figure 1D). Rats pretreated with Nuci-H showed significantly smaller infarct volumes than the MCAO group ($P < 0.001$), as rats pretreated with Nuci-M ($P < 0.05$) (Figure 1B,C). The quantitative statistical results of cerebral edema in all groups are shown in Figure 1D, which indicated that MCAO remarkably increased the cerebral water content (cerebral edema) compared to that in the sham group ($P < 0.001$). After treatment with Nuci-H and EGb 761, the cerebral water content was significantly reduced ($P < 0.05$).

https://dx.doi.org/10.1021/acsomega.0c05388
ACS Omega 2020, 5, 33433−33444

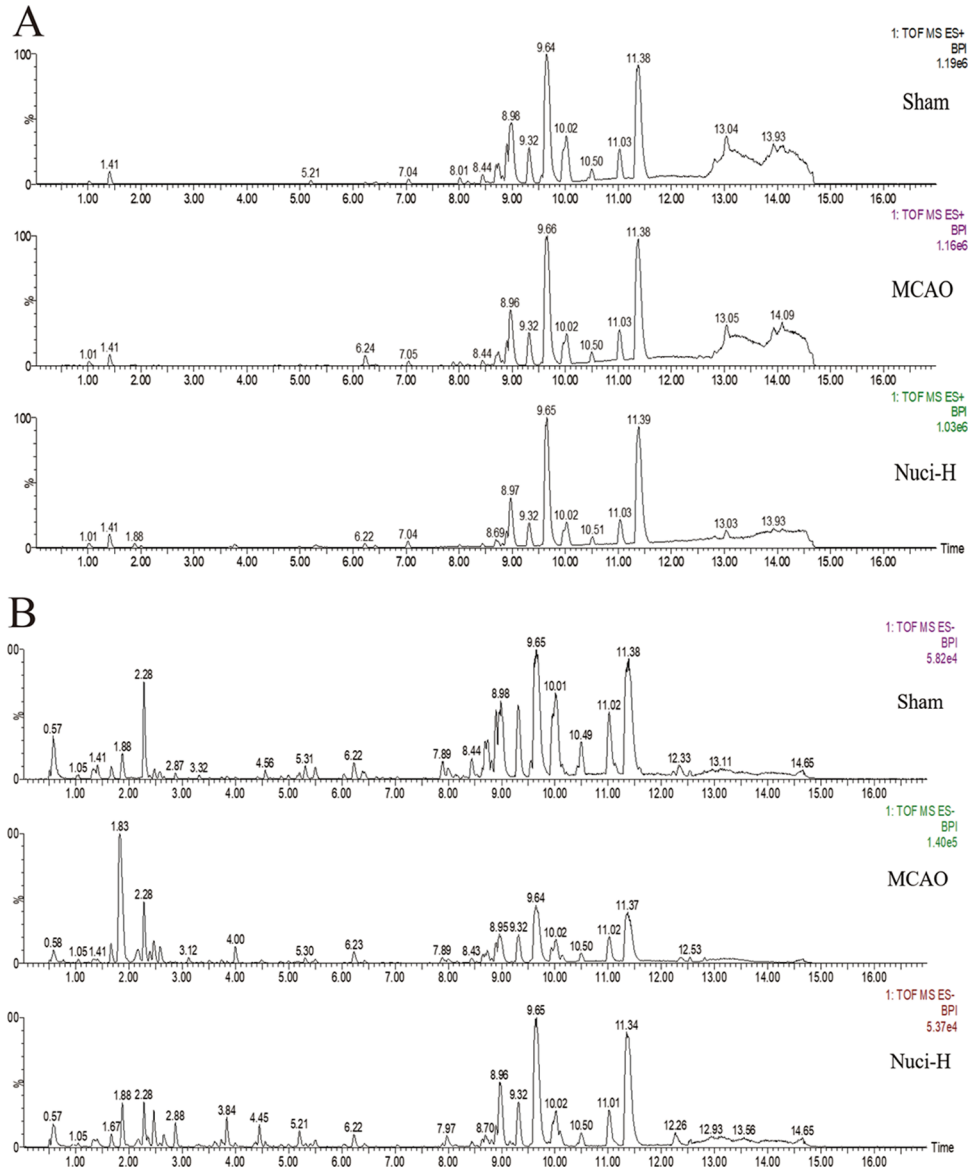

Figure 2. Representative base peak intensity (BPI) chromatograms of the rat serum from the treatment groups. The peaks were acquired via analyses of serum samples of different groups in positive (A) and negative (B) modes. (A) (ESI^+) and (B) (ESI^-) from top to bottom show the sham group, MCAO group, and Nuci-H group.

UPLC-Q-TOF/MS Analysis of Serum. According to the neurological deficit score, infarct volume, and cerebral water content results, the MCAO group, sham group, and Nuci-H group were selected for serum metabolomics analysis.

After MCAO model preparation and drug intervention, the levels of metabolites may change. Serum chromatograms were obtained using the UPLC-Q-TOF/MS system, including positive- and negative-ion modes. Figure 2A,B presents the positive- and negative-ion chromatograms, respectively, for the sham group, MCAO group, and Nuci-H group.

Metabolomics Profiling and Multivariate Statistical Analysis. To reveal the effects of nuciferine on the metabolic pattern of MCAO rats, the raw data of the sham group, MCAO group, and Nuci-H group were analyzed using principal component analysis (PCA) and orthogonal projections to latent structures discriminant analysis (OPLS-DA). The PCA mainly presents obvious clustering characteristics from the complex and multivariate results, which indicate certain differences in the levels of metabolites. The PCA score plots of the serum samples of the rats are shown in Figure 3A,B, and there was good separation among the sham, MCAO, and Nuci-H groups, which indicated that the MCAO model significantly disturbed the levels of endogenous metabolites and that nuciferine administration tended to correct the metabolite levels of MCAO rats.

To better elucidate the differences between groups and identify the endogenous biomarkers, we used the S-plot of the OPLS-DA model (Figure 3C−F). The relevant parameters of the OPLS-DA model in positive- and negative-ion modes were identified. Comparison of the sham and MCAO groups showed an $R^2Y = 0.9932$, $Q^2 = 0.9020$ and $R^2Y = 0.9682$, $Q^2 = 0.7091$, respectively, whereas the values for the Nuci-H group and MCAO group comparison were $R^2Y = 0.9884$, $Q^2 = 0.9695$, and $R^2Y = 0.9933$, $Q^2 = 0.9298$, respectively. The results indicated that the OPLS-DA model showed good stability and predictability. The farther away from the coordinate origin, the greater the contribution of the metabolites. Metabolites enclosed in the red quadrilateral

https://dx.doi.org/10.1021/acsomega.0c05388
ACS Omega 2020, 5, 33433−33444

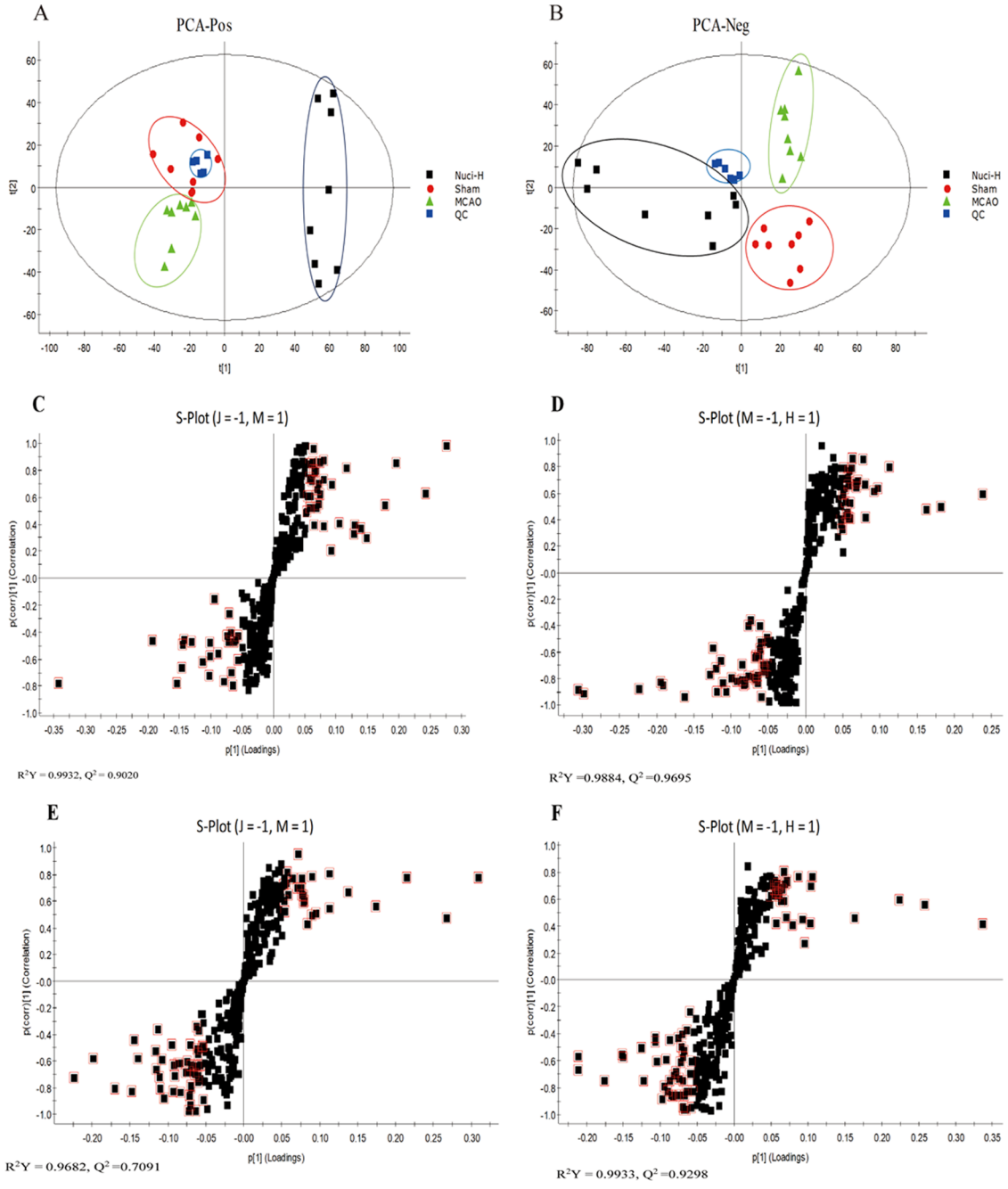

Figure 3. PCA score based on rat serum samples in the sham, MCAO, and Nuci-H groups, including ESI^+ (A) and ESI^- (B) modes. Every dot represents an animal, and the colors indicate different treatment groups. S-plot of OPLS-DA for the sham group versus the MCAO group, the MCAO group vs. the Nuci-H group in ESI^+ (C, D) and ESI^- (E, F) modes. The black square represents a different metabolite, and the red square indicates that this endogenous metabolite with variables with importance parameter (VIP) > 1 is closely related to stroke. The abbreviations (J, M, H) represent the sham group, MCAO group, and Nuci-H group, respectively (C−F).

Table 1. Surgical Procedures and Number of Rats Used in Various Treatments

	sham	MCAO	EGb 761	Nuci-L	Nuci-M	Nuci-H
neurological deficits infarct volume	n = 11	n = 11	n = 11	n = 11	n = 11	n = 11
brain water content	n = 11	n = 11	n = 11	n = 11	n = 11	n = 11
serum metabolomics	n = 8	n = 8				n = 8
total	n = 30	n = 30	n = 22	n = 22	n = 22	n = 30

indicated VIP > 1. The data of the OPLS-DA model derived from the sham group vs. the MCAO group and the MCAO group vs. the Nuci-H group were shown for ESI^+ (Figure 3C,D) and ESI^- (Figure 3E,F).

https://dx.doi.org/10.1021/acsomega.0c05388
ACS Omega 2020, 5, 33433−33444

Table 2. Information and Changing Trend of Potential Biomarkers in the Rat Serum[a,b]

no.	metabolite	t_R/min	mass-to-charge ratio	type	HMDB	KEGG	trend	
							MCAO/Sham	Nuci-H/MCAO
1	L-lactic acid	0.7254	89.0518	$[M-H]^-$	HMDB0000190	C00256	↑*	↓###
2	hydroxyphenylacetylglycine	1.371	208.0887	$[M-H]^-$	HMDB0000735	C05596	↓*	↓#
3	isobutyrylglycine	1.4258	144.0955	$[M-H]^-$	HMDB0000730	/	↑**	↓##
4	*N*-methylnicotinium	1.4638	176.067	$[M-H]^-$	HMDB0001009	/	↓*	↓#
5	N2-succinyl-L-ornithine	2.8724	231.1036	$[M-H]^-$	HMDB0001199	C03415	↓*	↓#
6	sebacic acid	3.315	201.0502	$[M-H]^-$	HMDB0000792	C08277	↑**	↓##
7	linoleic acid	4.8949	279.1474	$[M-H]^-$	HMDB0000673	C01595	↑***	↑###
8	tauroursodeoxycholic acid	5.1969	498.2942	$[M-H]^-$	HMDB0000874	/	↓*	↑#
9	sphingosine 1-phosphate	7.9323	378.2575	$[M-H]^-$	HMDB0000277	C06124	↓**	↑###
10	sphinganine 1-phosphate	8.2826	380.2727	$[M-H]^-$	HMDB0001383	C01120	↓***	↑###
11	2-hydroxyestradiol-3-methyl ether	9.9301	303.2521	$[M+H]^+$	HMDB0000380	/	↓**	↑###
12	glutamylphenylalanine	9.9338	293.2015	$[M-H]^-$	HMDB0029156	/	↓***	↓###
13	vitamin D2 3-glucuronide	10.4886	571.3343	$[M-H]^-$	HMDB0010344	/	↓***	↑###
14	neoxanthin	10.8794	599.3139	$[M-H]^-$	HMDB0003020	C08606	↓***	↑###
15	stearoylcarnitine	11.4485	428.3842	$[M+H]^+$	HMDB0000848	/	↓***	↑#
16	glucosylgalactosyl hydroxylysine	12.3866	485.2889	$[M-H]^-$	HMDB0000585	/	↑**	↑##
17	docosahexaenoic acid	12.5321	327.2532	$[M-H]^-$	HMDB0002183	C06429	↑*	↑##
18	petroselinic acid	12.8482	282.301	$[M+H]^+$	HMDB0002080	C08363	↓***	↑###
19	oxoglutaric acid	13.9886	144.952	$[M-H]^-$	HMDB0000208	C00026	↑***	↓###

[a]Note: *P < 0.05, **P < 0.01, ***P < 0.001 versus the sham group; #P < 0.05, ##P < 0.01, ###P < 0.001 versus the MCAO group. The treads of biomarkers were expressed with (↓) downregulated and (↑) upregulated. [b]FC > 1 showed that the content of metabolites in the MCAO group was higher than that in the sham group, and vice versa. Compared with the MCAO group, the situation of Nuci-H group was the same as above.

Analysis, Discovery, and Elucidation of Potential Biomarkers. Briefly, the following steps were used to identify metabolites in this investigation. The candidates were preliminarily screened using Progenesis QI software, and candidates with VIP > 1 from the OPLS-DA score plots were selected. The loading plot displayed potential MCAO-related metabolites according to their variable importance in projection (VIP) value, which was set to be higher than 1 (VIP > 1) and significant test, with P < 0.05. Based on the retention time and mass spectra with the authentic chemicals, some of the metabolites related to the MCAO-induced stroke injury were confirmed in rats (Table 1).

Nineteen metabolites were regarded as potential biomarkers of ischemic stroke in rat serum samples. The candidates were roughly divided into carboxylic acid compounds, such as L-lactic acid, oxoglutaric acid, linoleic acid, petroselinic acid, sebacic acid, tauroursodeoxycholic acid, *N*-methylnicotinium, vitamin D2 3-glucuronide, and stearoylcarnitine; amino acid metabolites, such as hydroxyphenylacetylglycine, glucosylgalactosyl hydroxylysine, isobutyrylglycine, N2-succinyl-L-ornithine, and glutamylphenylalanine; longer-chain polyunsaturated fatty acids and olefin compounds, such as neoxanthin, docosahexaenoic acid, and 2-hydroxyestradiol-3-methyl ether; and lipid compounds, such as sphingosine 1-phosphate and sphinganine 1-phosphate. The detailed information of the 19 differential metabolites (retention time, mass-to-charge ratio, HMDB, KEGG, trends, etc.) after MCAO preparation and nuciferine intervention is shown in Table 2.

Metabolic Pathway Analysis. Based on the results of pharmacodynamics and multidata analyses, biomarkers reflecting the treatment of nuciferine on stroke were determined. According to the identified metabolites, the metabolic networks were constructed using Cytoscape 3.7.2 software, which was conducive to better understand the internal correlation of the biomarkers in terms of the enzyme or gene levels and clearly demonstrate the relationship between the occurrence of stroke and the efficacy of nuciferine. The metabolic networks that were established based on the markedly different metabolites are shown in Figure 4. A total of seven stroke-related pathways were found in this study, which was labeled in the following figure and mainly involved: di-unsaturated fatty acid β-oxidation; glycine, serine, alanine, and threonine metabolism; glycolysis and gluconeogenesis; glycosphingolipid metabolism; linoleate metabolism; TCA cycle; urea cycle and metabolism of arginine, proline, glutamate, aspartate, and asparagine. Based on the discovery of the relevant biomarkers and determined metabolic pathways in the metabolic networks, we have elaborated the anti-stroke molecular mechanisms of nuciferine in our research (Figure 5). The identified metabolites contributed to the information of the metabolic pathways (Table S1).

Cytoscape to Explore the Metabolite−Protein Network. Subsequently, to further explore the intrinsic relationship between the potential biomarkers and potential proteins, the networks involved in some categories (genes, enzymes, etc.) were also discovered using Cytoscape 3.7.2.[31] Approximately 93 genes were found. These genes were imported into an online database for analysis (http://ci.smu.edu.cn/GenCLiP2/analysis.php#). A total of 11 proteins were confirmed as follows: PLA2, 12/15-LOX, SPHK1, SPHK2, IDH, GOT1, AGXT2, CYP2B, FADS, DLDH, and GPT. The details with abbreviations and full names of proteins considered as potential markers for MCAO-induced stroke and the role of nuciferine are shown in Table 3.

DISCUSSION

Ischemic cerebral stroke is the second leading cause of death and carries a tremendous public health burden, especially in developing countries. It results in a mortality rate of approximately 30%,[32,33] and its costs account for approximately 3−7% of total national health care expenditures.[34,35] Stroke is a multifactorial and complex pathophysiological

https://dx.doi.org/10.1021/acsomega.0c05388
ACS Omega 2020, 5, 33433−33444

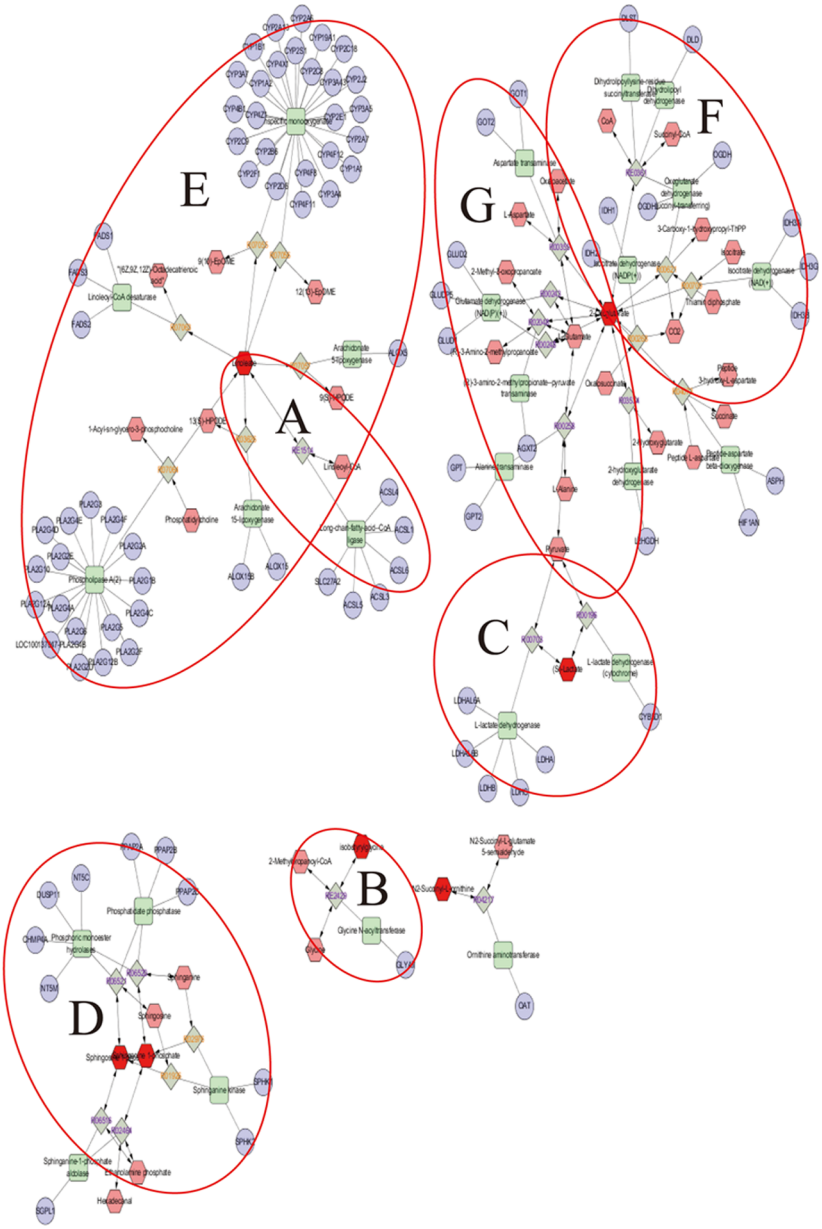

Figure 4. Metabolic correlation network analysis. Metabolomics pathways were discovered and determined using Cytoscape 3.7.2. Hexagon, metabolites; round rectangle, enzyme; ellipse, gene; and diamond, reaction. Di-unsaturated fatty acid β-oxidation metabolism; glycine, serine, alanine, and threonine metabolism; and glycolysis and gluconeogenesis metabolism are shown in (A, B), and C, respectively. Sphingosine kinases (SphK1 and SphK2) and sphingosine 1-phosphate (S1P) are involved in glycosphingolipid metabolism (D). (E) represents the linoleate metabolism. F shows that certain enzymes and metabolites participated in the TCA cycle, such as isocitrate dehydrogenase enzymes (IDH) and oxoglutaric acid. Glutamate oxaloacetate transaminase (GOT) and glutamate-pyruvate transaminase (GPT) were also involved in the urea cycle and metabolism of arginine, proline, glutamate, aspartate, and asparagine metabolism (G). The original unprocessed and high-resolution (this figure) data are shown in Figure S1.

process. The specific pathogenesis is not clear, and the available drugs are not ideal. The present study confirmed that nuciferine, a bioactive monomer extract from *Nymphaea caerulea* and *Nelumbo nucifera* Gaertn, could significantly improve the ethological aspect of rats with cerebral ischemia. However, the molecular mechanism has not been elucidated, which hindered the progress of anti-stroke research. Metabolomics is a systematic method that contributes to the study of the possible therapeutic mechanisms of drugs. These facts encouraged us to use the UPLC-Q-TOF/MS-based serum metabolomics method to study the metabolic responses and the metabolic pathways of rats after intervention with nuciferine. After that, the relevant biomarkers and pathways in the metabolic networks were discovered (Figure 5). This provides a new idea for us to explore the anti-stroke molecular mechanisms of nuciferine.

In this study, a metabolomics method was used to analyze the serum samples of MCAO model rats, a total of 12 endogenous metabolites were identified in the serum of MCAO-induced rats. The increase or decrease of the metabolites content in the serum of rats caused the disorder of the corresponding biological metabolic pathways, indicating that MCAO caused the metabolic disorder of the body and induced the occurrence of cerebral ischemic diseases. After

https://dx.doi.org/10.1021/acsomega.0c05388
ACS Omega 2020, 5, 33433−33444

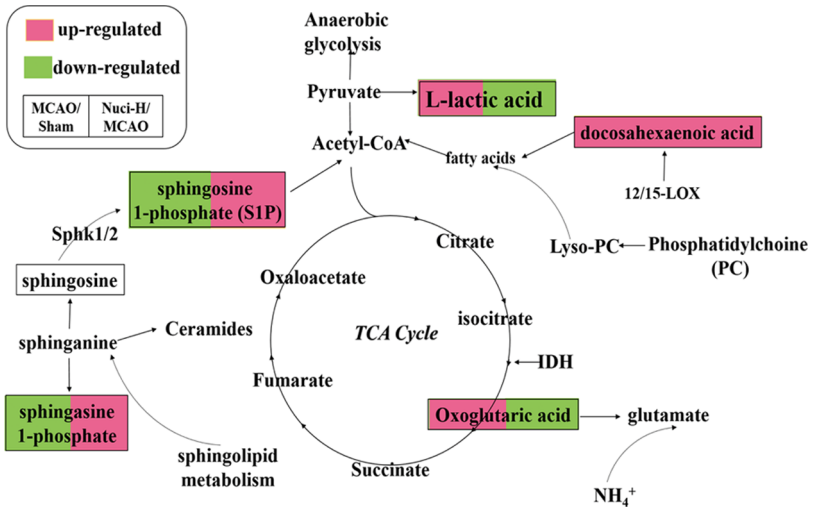

Figure 5. Schematic diagram of the perturbed metabolic pathways that were detected by the UPLC/MS/MS, showing the network links between the identified biomarker pathways and MCAO-induced ischemic stroke. The red metabolites were upregulated, while the green metabolites were downregulated in the Nuci-H group compared to the MCAO group.

Table 3. Full Names of the Potential Protein Targets[a]

name abbreviation	full name
PLA2	phospholipase A2
12/15-LOX	12/15-lipoxygenase
SPHK1	sphingosine kinase 1
SPHK2	sphingosine kinase 2
IDH	isocitrate dehydrogenase enzymes
GOT1	glutamate oxaloacetate transaminase 1
AGXT2	alanine-glyoxylate aminotransferase 2
CYP2B	cytochrome P450 2B
FADS	fatty acid desaturase
DLDH	dihydrolipoamide dehydrogenase
GPT	glutamate-pyruvate transaminase

[a]These targets in serum are the targets after administration and related to MCAO.

nuciferine administration, the contents of L-lactic acid, tauroursodeoxycholic acid, docosahexaenoic acid, oxoglutaric acid, sphinganine 1-phosphate, and sphingosine 1-phosphate could be recalled, mainly involved in energy metabolism, sphingolipid metabolism, and anti-inflammatory and anti-apoptotic processes. Eventually, nuciferine can regulate the normal physiological metabolism level of rats, thereby exerting anti-cerebral ischemic effects.

Macroscopic Analysis and Other Metabolites and Enzymes. At this stage of research, the MCAO model was established, and the protective effects of nuciferine against cerebral ischemia were evaluated. Numerous studies have shown that the MCAO model is consistent with the pathogenesis of human stroke, and it possesses the advantages of good repeatability and high stability, which provides a powerful tool for the study of ischemic encephalopathy mechanism and drug screening.[36] Weakness of the contralateral limbs is the most important symptom of stroke.[37] We performed the initial evaluation of the nuciferine treatment using neurological scores. Compared to the MCAO group, the neurological function scores of the rats in the EGb 761 group and the Nuci-H group were significantly reversed, and the rats could almost crawl normally, which indicated that a sufficient concentration of nuciferine repaired the embolism-induced movement disorders.

The MCAO thread ligation model causes behavioral and physiological abnormalities in rats, which may be related to the decrease in cerebral blood flow (CBF), which disrupts the balance in the brain. Huang et al.[38] found that an inflammatory response or cytokines (TNF-α and IL-1α/β) were initiated when cerebral stroke occurred, and vice versa. Edema and infarct volume, which are consistent with the above factors, are the most obvious pathological manifestations of stroke. Our current data demonstrated that nuciferine attenuated the increase in infarct volume and brain edema (Figure 1B–D). Dispersants and protections are produced by 12/15-LOX from the longer-chain polyunsaturated fatty acid docosahexaenoic acid,[39] which are effective anti-inflammatory compounds that may limit inflammation-induced brain damage.[40] The expression of some proteins (PLA2, 12/15-LOX) alters metabolites and the di-unsaturated fatty acid β-oxidation metabolism that contributes to the alleviation of the characteristics of stroke injury. The above results showed that nuciferine regulated the levels of endogenous metabolites associated with the release of inflammatory cytokines and achieved the anti-stroke effects via inhibition of the occurrence of inflammation, which provided some ideas to support our examination of nuciferine treatment of cerebral ischemic stroke in the future.

Biomarkers Obtained and Discussion of Sphingolipid Metabolism. Sphingolipids (including sphingosine and sphinganine) are critical mediators of neuronal cell death, proliferation, and migration, which are related to ischemic stroke.[41,42] Sphinganine may be converted to ceramides, sphingosine, and sphingosine 1-phosphate (S1P). Several studies have provided evidence that S1P is an immunomodulatory factor.[43] Sphingosine plays a neuroprotective role only when it is phosphorylated and transformed into endogenous S1P. Sphingosine kinases (SphK1 and SphK2) are the rate-limiting enzymes that convert sphingosine into S1P.[44] Blondeau et al.[45] and Wacker et al.[46] found that the level of Sphk2, but not Sphk1, is increased by stroke. Pfeilschifter et al.[47] identified larger infarcts in Sphk2-deficient mice compared to those with normal levels. Increasing evidence suggests that the Sphk2/S1P axis acts as an indispensable mediator of stroke.

https://dx.doi.org/10.1021/acsomega.0c05388
ACS Omega 2020, 5, 33433−33444

The content of S1P was significantly reduced in the MCAO group in our study, which may be related to the inhibition of SphK2 activity. Notably, S1P was reversed after the administration of nuciferine. MCAO may restrain SphK activity and reduce the concentrations of synthetic S1P to cause an imbalance of material metabolism (glycosphingolipid metabolism), which results in stroke symptoms.

Energy Metabolism. The brain has the most vigorous energy metabolism of any organ, but it does not store energy. When blood vessels are blocked, cerebral blood flow decreases and oxygen delivery is restricted, which initiate anaerobic glycolysis to produce a small amount of ATP to provide energy to the brain, and it results in an accumulation of hydrogen ions.[48] Compensatory mechanisms are initiated, glycogen is quickly depleted, and a large amount of lactic acid is produced.[49] Lactic acid is a marker product of anaerobic glucose fermentation. Lactic acid and its synergistic acid effect (hydrogen ion enrichment) are important factors in neuronal damage in brain injury. In this experiment, after MCAO intervention, the content of L-lactic acid was increased, and the level of L-lactate in the Nuci-H group was extremely significantly decreased ($P < 0.001$). L-lactic acid reflects the degree of the ischemic core area, which is consistent with the cerebral infarction volume with the trend of L-lactate. These data demonstrated that the neuroprotective function of nuciferine on stroke occurred via the correcting of the abnormal energy metabolism pattern, which was related to the tricarboxylic acid (TCA) cycle and resulted in the reduced rate of infarct and the death of neurons.

The conversion of glucose to pyruvate is a common process. Oxoglutaric acid is produced under the action of pyruvate dehydrogenase and isocitrate dehydrogenase enzymes (IDH), and it is the precursor of glutamate synthesis. Therefore, the trend of oxoglutaric acid can indirectly indicate the content of excitatory amino acids. Our data revealed that the levels of oxoglutaric acid, a TCA cycle intermediate, were obviously increased in the MCAO group ($P < 0.001$), which may indicate that energy production was disordered in MCAO rats. Surprisingly, oxoglutaric acid showed a downward trend in the Nuci-H group. These results indicated that brain protection against stroke in MCAO rats occurred via improved energy metabolism and anti-glutamate excitotoxicity.[50]

Further, we conclude that anaerobic glycolysis (lactic acid) and TCA cycle (oxoglutaric acid) indicators were affected, which are directly related to energy metabolism. These results indicate that the therapeutic effects of nuciferine on cerebral ischemia are partially due to its ability to repair energy metabolism.

Other Metabolisms. Tauroursodeoxycholic acid (TUDCA), an endogenous hydrophilic bile acid, which is formed by the conjugation of ursodeoxycholic acid (UDCA) with taurine.[51] TUDCA exhibits anti-inflammatory effects and attenuates neuronal loss (apoptosis) in neurodegenerative diseases.[52] The possible neuroprotective mechanisms of TUDCA is inhibiting apoptosis by modulating Bcl-2, BAX, and caspase activation.[53] Apoptosis plays a vital role in maintaining homeostasis, physiological processes, and many diseases.[54] Rodrigues et al.[55] investigated that TUDCA could alleviate brain injury by inhibiting the expression of Caspase-3 in MCAO rats. In our study, the concentrations of TUDCA were obviously decreased in the MCAO group. This result may indicate that apoptotic destroys the neural cell structure, resulting in the symptoms of stroke. After nuciferine treatment, the level of TUDCA could significantly increase.

Nuciferine downregulated L-lactic acid, isobutyrylglycine, sebacic acid, hydroxyphenylacetylglycine, N-methylnicotinium, N2-succinyl-L-ornithine, glutamylphenylalanine, and oxoglutaric acid, and it upregulated tauroursodeoxycholic acid, sphingosine 1-phosphate, sphinganine 1-phosphate, 2-hydroxyestradiol-3-methyl ether, vitamin D2 3-glucuronide, neoxanthin, stearoylcarnitine, petroselinic acid, linoleic acid, glucosylgalactosyl hydroxylysine, and docosahexaenoic acid in rat serum. It is worth exploring the activity of certain genes and enzymes related to stroke occurrence and metabolites, such as PLA2, 12/15-LOX, SPHK, IDH, GOT1, CYP2B, FADS, and GPT, which are highly relevant to nuciferine, in further investigations.

CONCLUSIONS

The complex and incompletely clear pathogenesis of stroke, accompanied by serious and irreversible sequelae such as deformity, language dysfunction, and dementia, hinder the progress in global medical treatment of this disease. Although several therapeutic methods have been developed for key pathophysiological targets, these treatments are not ideal. The present study examined the protective effects of nuciferine on ischemic stroke using a metabolomics approach based on UPLC-Q-TOF/MS for the first time. Twelve metabolites closely associated with MCAO-induced stroke rats were identified. Moreover, we focused on the effects of nuciferine in MCAO rats. The neurological function scores evaluated the anti-ischemic effect of nuciferine using behavioral testing, and infarct volume and cerebral water content were investigated to evaluate the pharmacodynamic effects. After oral administration of nuciferine, the behavioral and pharmacodynamic indicators tended toward or returned to normal levels and restored the metabolic disturbances.

Overall, our results demonstrated that sphingolipid metabolism, metabolic stress, energy metabolism (glycolysis and gluconeogenesis and TCA cycle), and other metabolisms were the notable involved pathways whose modulation may prevent suffering from the occurrence of stroke. After drug intervention, it was shown that nuciferine can regulate the body's metabolic balance by exerting neuroprotective, antiapoptotic, and anti-inflammatory effects, thereby playing an anti-stroke effect. These findings provide a basis for the study of nuciferine for the treatment of stroke.

MATERIALS AND METHODS

Chemicals and Reagents. Nuciferine (Nuci) was purchased from Sigma-Aldrich (Burlington, MA) (purity ≥ 98%; Shanghai, China). The positive control was EGb 761 (Chinese National Medicine permission number: H2O140768), which was researched and manufactured by Dr. Willmar Schwabe Pharmaceuticals Co., Ltd. (Germany). Chloral hydrate and carboxymethylcellulose sodium (CMC-Na) were purchased from Beijing BioDee Biotechnology Co., Ltd. (Beijing, China). Formic acid and acetonitrile were acquired from Fisher Co. Ltd. (Pittsburgh, PA). Double-distilled water was provided by a Milli-Q system (Millipore, MA).

Experimental Animals. Adult male Sprague-Dawley (SD) rats weighing 240−270 g were purchased from Beijing Vital River Laboratory Animal Technology Co., Ltd. (Beijing,

https://dx.doi.org/10.1021/acsomega.0c05388
ACS Omega 2020, 5, 33433−33444

China) and kept in propylene cages for adaptation periods of 3 days at a temperature of 25 ± 2 °C, a relative humidity of 45 ± 15%, and a 12 h light−dark cycle and fed freely. The China Academy of Chinese Medical Science's Administrative Panel on Laboratory Animal Care approved all of the experimental procedures, which followed the guidelines on experimental design and analysis in pharmacology. Every effort was made to minimize the suffering of animals.

Animal Groups and Model Establishment. After adaptive feeding, all male rats were randomly divided into six groups (n = 11): the sham group, the MCAO group, the positive control group (EGb 761), and the low-, middle- and high-dose nuciferine treatment groups (Nuci-L, Nuci-M, and Nuci-H, respectively). The number of rats used in various treatments are shown in Table 1. The nuciferine doses given were 10, 20, and 40 mg/kg, respectively.

The rats were anesthetized with 10% chloral hydrate (350 mg/kg), and the MCAO model was established as previously indicated.[23−25] The surgeries were performed after the response to the noxious stimulus disappeared and breathing, body temperature, and other normal physiological conditions stabilized.[26] Briefly, the animals were attached to the operating board with the abdomen upward, and the origin of the MCA was occluded via the insertion of a 4−0 single nylon suture with a round head into the internal carotid artery from the left external carotid artery.[27] The surgical site was closed with a degradable surgical suture after disinfection. The sham group underwent the same surgical experimental procedure without filament insertion.

The entire modeling process ensured that the experimenters and the environment were consistent. All treatment groups were assigned in a randomized manner.

Dosing Regimens. Considering the low solubility of nuciferine, an equal amount of carboxymethylcellulose (CMC-Na) was added, and ultrasound-assisted dissolution was used. The sham and MCAO groups were fed an equivalent volume of 5% CMC-Na water solution. The three nuciferine treatment groups were 10, 20, and 40 mg/kg. The EGb 761 group was treated with 100 mg/kg. All treatments were given intragastrically within 30 min before surgery.

Evaluation of Neurological Deficits. After surgery, the rats were carefully placed in cages. The experimenters observed that all animals woke normally, and rats that died after surgery were recorded and excluded. Behavioral scoring was performed 24 h after MCAO, and a single researcher who was not aware of the experimental group assignments performed the entire process. The behaviors were scored on a five-point scale (0−4 points) as described previously.[28]

Evaluation of Cerebral Infarct Volume. After the neurological function scoring was completed, the rats were anesthetized via intraperitoneal injection and brain tissues were collected and washed with a physiological saline solution. The intact brain tissues were stored in a flat dish at −20 °C and removed after completely hardening. Then, the tissues were carefully cut into six 2 mm thick coronal sections and stained with 2% TTC at room temperature until a red/white color boundary appeared. A digital camera was used to record the stained brain slices. Brain slice data were quantitatively analyzed using ImagePro Plus 6.0 to measure the infarct volume.

Quantification of Brain Water Content. The effects of nuciferine on the rate of postoperative brain edema was evaluated via measurement of the cerebral water content. Two fresh hemispheres were separately weighed and recorded. The water content was calculated as follows: cerebral water content = (left brain − right brain)/(left brain + right brain) × 100%. The infarction cerebral hemisphere was the left brain.

Serum Sample Collection and Handling for Metabolomics Analysis. After successfully establishing the MCAO model, whole blood of all rats (3−5 mL) was collected from the abdominal aorta and placed in a centrifuge tube. The blood samples were numbered and left to stand on ice for 30 min. Then, they were centrifuged at 3500 g for 15 min at 4 °C. The supernatant serum was carefully removed using a pipette, placed in a new EP tube, and then stored at −20 °C for approximately 20 min. The serum samples were stored at −80 °C for further metabolic analysis.

Prior to UPLC-Q-TOF/MS detection, the serum sample was removed from the refrigerator and thawed at room temperature. A volume of 150 μL of serum was transferred to a new tube, and 450 μL of acetonitrile was added to precipitate the protein. The above mixture (600 μL) was vortexed and centrifuged sequentially at 2000 rpm for 10 min and then 13 000 rpm for 10 min at 4 °C. The supernatant (400 μL) was transferred to a new EP tube and evaporated to dryness under a steady nitrogen flow in the fume hood. Residues were redissolved in 100 μL of 10% acetonitrile, followed by vortexing and centrifugation. The supernatant was collected again. The supernatant (80 μL) was injected into a sampling bottle for metabolomics analysis. Due to the characteristics of the sample, the entire process was carried out on ice.

Quality Control Sample. To evaluate the stability and repeatability of the UPLC-Q-TOF/MS analysis system, 10 μL of the supernatants of every serum samples from each group were selected and mixed as a pooled quality control (QC) sample. QC samples were handled as same as serum samples. One QC sample was analyzed after every 10 test samples to check the stability and performance of the instrument.

UPLC-Q-TOF/MS Analysis. During the course of this experimental study, metabolomics analysis was performed using a Synapt G2 UPLC-Q-TOF/MS (Waters Corporation, Milford, MA) system. The chromatographic separation (UPLC) conditions are shown below. An Acquity UPLC HSS C_{18} column (1.7 μm, 2.1 × 100 mm^2) was used with an injection volume of 4 μL. The column temperature and flow rate were maintained at 40 °C and 0.4 mL/min, respectively. The mobile phases of serum samples consisted of 0.1% formic acid−water (solvent A) and 0.1% formic acid−acetonitrile (solvent B). Notably, the standard elution program conditions were as follows: 0−1.5 min with 10−20% B; 1.5−4 min with 20−40% B; 4−13 min with 40−90% B; 13.1−14 min with 90% B; and 14.1−17 min with 10% B.

The UPLC-Q-TOF/MS acquisition was used in the MSe mode. This mode can scan the primary and secondary mass spectra simultaneously. Mass spectrometry (MS) analysis was performed in positive- and negative-ion modes equipped with an electrospray ionization (ESI) source. Leucine−enkephalin (ESI^+, m/z 556.2771; ESI^-, m/z 554.2615) was used as a standard for quality determination and lock mass solution. The following final MS conditions were used in the positive-ion detection mode: capillary voltage, 2.7 kV; source temperature, 120 °C; desolvation temperature, 500 °C; cone gas flow, 50 L/h; desolvation gas flow, 800 L/h; low collision energy for precursors, 25 V; high energy for fragment ions, 50 V. The same detection method was used for both the negative ion and positive ion, except that the negative ion was under 2.1 kV

https://dx.doi.org/10.1021/acsomega.0c05388
ACS Omega 2020, 5, 33433−33444

capillary voltage. The mass spectrum collected and analyzed ranged from 50 to 1000 m/z.

Multivariate Data Analysis. According to the above methodology, the raw data were obtained from the UPLC-Q-TOF/MS system, which were processed and analyzed in Progenesis QI (Waters Corporation, Milford, MA), including nonlinear retention time alignment, peak discrimination, filtering, alignment, matching, and identification. The parameters for each ion primarily included the retention time and mass-to-ratio data pairs. Unit variance scaling and the mean-centered method were used to handle data, followed by multivariate analysis including principal component analysis (PCA), which revealed the aggregation and dispersion of samples. An orthogonal partial least-squares discriminate analysis (OPLS-DA) algorithm was further constructed using the permutation test to prevent overfitting. OPLS-DA showed differences between two groups. The OPLS-DA score plots were described using the cross-validation parameters R^2Y and Q^2, where R^2Y indicates the goodness of fit of the model, and Q^2 estimates its prediction ability.[29] The variable importance in the projection (VIP) values, which expresses the significance in discriminating between groups, were used to select the biomarkers. The present study selected VIP > 1 in the OPLS-DA model, which were identified as potential variables. The average peak area of metabolites between the two groups (FC) was used to judge the change in the metabolite content between different groups. FC > 1 indicated that the content of the metabolite increases, whereas FC < 1 indicated that the content decreases. After that, P values were obtained and the metabolites were determined in the next step. Finally, when $P < 0.05$ and VIP > 1, the metabolites were considered statistically significant.[30]

The other statistical (pharmacodynamic statistical) analyses performed were processed using SPSS 17.0 (SPSS Inc., USA). The values are presented as mean ± standard deviation (SD). The difference among the groups was compared primarily using one-way analysis of variance (ANOVA) followed by Fisher's post hoc test. Neurological deficit data were collected using the Kruskal–Wallis test. $P < 0.05$ was considered statistically significant, and differences were considered extremely significant when $P < 0.01$ or 0.001.

Biomarker Identification, Metabolic Pathway, and Protein Correlation Analysis. The possible metabolites were screened and identified using certain online databases, such as the Human Metabolome Database (http://www.hmdb.ca/), METLIN (http://metlin.scripps.edu), and SMPD (http://www.smpdb.ca/). The spectra were compared with the MS/MS information from the above databases to verify the structure of the putative metabolites. The metabolites were identified via comparison of the retention times and fragments of metabolites with the reference samples. The identified potential biomarkers were transferred to Cytoscape 3.7.2. The pathways and metabolite-correlation protein network were constructed using Cytoscape 3.7.2 and GeneCards (https://www.genecards.org/), which were also used to acquire potential protein targets of nuciferine. Protein targets related to biomarkers were identified using Cytoscape, and the potential protein targets were predicted using GeneCards.

■ ASSOCIATED CONTENT

Supporting Information

The Supporting Information is available free of charge at https://pubs.acs.org/doi/10.1021/acsomega.0c05388.

Original unprocessed and high-resolution metabolic correlation network analysis (Figure S1) and metabolites and their related metabolic pathways (Table S1) (PDF)

■ AUTHOR INFORMATION

Corresponding Authors

Binyu Wen − *Dongfang Hospital, Beijing University of Chinese Medicine, Beijing 100078, P. R. China;* orcid.org/0000-0002-7549-1508; Phone: +010-67689634; Email: wenbinyu@163.com

Zhiyong Yan − *School of Life Science and Engineering, Southwest Jiao Tong University, Chengdu 610031, Sichuan, P. R. China*; Phone: +86-28-87601838; Email: yzhiy@swjtu.edu.cn; Fax: +86-28-87603202

An Liu − *Key Laboratory of Beijing for Identification and Safety Evaluation of Chinese Medicine, Institute of Chinese Materia Medica, China Academy of Chinese Medical Sciences, Beijing 100700, P. R. China*; Phone: +86-10-64093381; Email: aliu@icmm.ac.cn; Fax: +86-10-64013996

Authors

Lanlan Wu − *Key Laboratory of Beijing for Identification and Safety Evaluation of Chinese Medicine, Institute of Chinese Materia Medica, China Academy of Chinese Medical Sciences, Beijing 100700, P. R. China; School of Life Science and Engineering, Southwest Jiao Tong University, Chengdu 610031, Sichuan, P. R. China;* orcid.org/0000-0002-8363-007X

Chang Chen − *Key Laboratory of Beijing for Identification and Safety Evaluation of Chinese Medicine, Institute of Chinese Materia Medica, China Academy of Chinese Medical Sciences, Beijing 100700, P. R. China*

Yongbiao Li − *Key Laboratory of Beijing for Identification and Safety Evaluation of Chinese Medicine, Institute of Chinese Materia Medica, China Academy of Chinese Medical Sciences, Beijing 100700, P. R. China; School of Life Science and Engineering, Southwest Jiao Tong University, Chengdu 610031, Sichuan, P. R. China*

Cong Guo − *Key Laboratory of Beijing for Identification and Safety Evaluation of Chinese Medicine, Institute of Chinese Materia Medica, China Academy of Chinese Medical Sciences, Beijing 100700, P. R. China*

Yuqing Fan − *Key Laboratory of Beijing for Identification and Safety Evaluation of Chinese Medicine, Institute of Chinese Materia Medica, China Academy of Chinese Medical Sciences, Beijing 100700, P. R. China; School of Life Science and Engineering, Southwest Jiao Tong University, Chengdu 610031, Sichuan, P. R. China*

Dingrong Yu − *Key Laboratory of Beijing for Identification and Safety Evaluation of Chinese Medicine, Institute of Chinese Materia Medica, China Academy of Chinese Medical Sciences, Beijing 100700, P. R. China*

Tinglan Zhang − *Key Laboratory of Beijing for Identification and Safety Evaluation of Chinese Medicine, Institute of Chinese Materia Medica, China Academy of Chinese Medical Sciences, Beijing 100700, P. R. China; School of Life Science and Engineering, Southwest Jiao Tong University, Chengdu 610031, Sichuan, P. R. China*

Complete contact information is available at: https://pubs.acs.org/10.1021/acsomega.0c05388

https://dx.doi.org/10.1021/acsomega.0c05388
ACS Omega 2020, 5, 33433−33444

Author Contributions

L.W. and C.C. contributed equally to this work. L.W., A.L., and Z.Y. conceptualized this work; B.W. and C.C. were involved in methodology and validation, respectively; Y.L. and C.G. conducted formal analysis; L.W. carried out the investigation; C.C., A.L., and Z.Y. were responsible for resources; L.W. and B.W. were involved in data curation; L.W. wrote and prepared the original draft; L.W. and C.C. were responsible for writing, review, and editing; Y.L., Y.F., and T.Z. contributed to visualization; Y.F., D.Y., and T.Z. supervised the work; L.W. and C.C. were involved in project administration; and A.L. and Z.Y. were responsible for funding acquisition. All authors read and approved the final manuscript.

Author Contributions

[#]L.W. and C.C. contributed equally to this work.

Notes

The authors declare no competing financial interest.

■ ACKNOWLEDGMENTS

This work was supported by the Key Project of Research and Development Plan of Science and Technology Department of Sichuan Province (2018SZ0078) and the Major Scientific and Technological Special Project for "Significant New Drugs Creation" (nos. 2019ZX09201005 and 2018YFC1706503). The authors are grateful to these institutions for the financial support.

■ REFERENCES

(1) Go Alan, S. Mozaffarian Dariush.Heart disease and stroke statistics–2014 update: a report from the American Heart Association. *Circulation* **2014**, *129*, e28−e292.

(2) Wang, X. G.; Zhu, D. D.; Li, N.; Huang, Y. L.; Zhao, J.; et al. Scorpion Venom Heat-Resistant Peptide is Neuroprotective against Cerebral Ischemia-Reperfusion Injury in Association with the NMDA-MAPK Pathway. *Neurosci. Bull.* **2020**, *36*, 243−253.

(3) Pénzes, M.; Túrós, D.; Máthé, D.; Szigeti, K.; Málnási-Csizmadia, A.; et al. Direct myosin-2 inhibition enhances cerebral perfusion resulting in functional improvement after ischemic stroke. *Theranostics* **2020**, *10*, 5341−5356.

(4) Eltzschig, H. K.; Eckle, T.; Eltzschig, H. K.; Eckle, T. Ischemia and reperfusion-from mechanism to translation. Nat Med 17: 1391-1401. *Nat. Med.* **2011**, *17*, 1391−1401.

(5) Grabowska-Fudala; Barbara; Jaracz; Krystyna; Gorna; Miechowicz; Izabela; Wojtasz; Jan; Kazmierski. Depressive symptoms in stroke patients treated and non-treated with intravenous thrombolytic therapy: a 1-year follow-up study. *J. Neurol.* **2018**, *265*, 1897−1899.

(6) Luo, X.; Chen, X.; Shen, X.; Yang, Z.; Du, G. Rapid identification and analysis of the active components of traditional Chinese medicine Xiaoxuming decoction for ischemic stroke treatment by integrating UPLC-Q-TOF/MS and RRLC-QTRAP MS n method. *J. Chromatogr. B* **2019**, *1124*, 313−322.

(7) Jiang, C.; Xu, Y. C.; Zhang, W.; Pan, W.; Chao, X. Effects and safety of Buyang-Huanwu Decoction for the treatment of patients with acute ischemic stroke: A protocol of systematic review and meta-analysis. *Medicine* **2020**, *99*, No. e20534.

(8) Li, J.; Chen, Z.; Zhang, X.; et al. Bioactive components of Chinese herbal medicine enhance endogenous neurogenesis in animal models of ischemic stroke: A systematic analysis. *Medicine* **2016**, *95*, No. e4904.

(9) Liu, M.; Liu, X.; Wang, H.; et al. Metabolomics study on the effects of Buchang Naoxintong capsules for treating cerebral ischemia in rats using UPLC-Q/TOF-MS. *J. Ethnopharmacol.* **2016**, *180*, 1−11.

(10) Wang, M.; Mingjiang, Y.; Liu, J.; Norio, T.; Fangze, T. Ligusticum chuanxiong exerts neuroprotection by promoting adult neurogenesis and inhibiting inflammation in the hippocampus of ME cerebral ischemia rats. *J. Ethnopharmacol.* **2019**, *249*, No. 112385.

(11) Fu, D.; Li, J.; Shi, Y.; Zhang, X.; Lin, Y.; Zheng, G. Sanhua Decoction, a Classic Herbal Prescription, Exerts Neuroprotection Through Regulating Phosphorylated Tau Level and Promoting Adult Endogenous Neurogenesis After Cerebral Ischemia/Reperfusion Injury. *Front. Physiol.* **2020**, *11*, 57.

(12) Lu, L.; Li, H.-Q.; Liu, A.-J.; Li, J.-H.; Zheng, G.-Q. Neuroprotection of Sanhua Decoction against Focal Cerebral Ischemia/Reperfusion Injury in Rats through a Mechanism Targeting Aquaporin 4. *Evidence-Based Complementary Altern. Med.* **2015**, *2015*, No. 584245.

(13) Zhou, L.; Wang, Q.; Zhang, H.; Li, Y.; Xu, M.; Xie, S. YAP Inhibition by Nuciferine via AMPK-Mediated Downregulation of HMGCR Sensitizes Pancreatic Cancer Cells to Gemcitabine. *Biomolecules.* **2019**, *9*, No. 620.

(14) Fuchuan, G.; Xue, Y.; Xiaoxia, L.; Rennan, F.; Chunmei, G.; Yanwen, W.; Ying, L.; Changhao, S.; Avila, M. A. Nuciferine Prevents Hepatic Steatosis and Injury Induced by a High-Fat Diet in Hamsters. *PLoS One* **2013**, *8*, No. e63770.

(15) Wang, M. X.; Zhao, X. J.; Chen, T. Y.; Liu, Y. L.; Jiao, R. Q.; Zhang, J. H.; Ma, C.; Liu, J. H.; Pan, Y.; Kong, L. D. Nuciferine Alleviates Renal Injury by Inhibiting Inflammatory Responses in Fructose-Fed Rats. *J. Agric. Food Chem.* **2016**, 7899−7910.

(16) Agnihotri, V. K.; Elsohly, H. N.; Khan, S. I.; Jacob, M. R.; Joshi, V. C.; Smillie, T.; Khan, I. A.; Walker, L. A. Constituents of Nelumbo nucifera leaves and their antimalarial and antifungal activity. *Phytochem. Lett.* **2008**, *1*, 89−93.

(17) Jung, H. A.; Jin, S. E.; Choi, R. J.; Kim, D. H.; Kim, Y. S.; Ryu, J. H.; Kim, D. W.; Son, Y. K.; Park, J. J.; Choi, J. S. Anti-amnesic activity of neferine with antioxidant and anti-inflammatory capacities, as well as inhibition of ChEs and BACE1. *Life Sci.* **2010**, *87*, 420−430.

(18) Xiao, J. H.; Zhang, J. H.; Chen, H. L.; Feng, X. L.; Wang, J. L. Inhibitory effects of isoliensinine on bleomycin-induced pulmonary fibrosis in mice. *Planta Med.* **2005**, *71*, 225−230.

(19) Wang, X.; Cheang, W. S.; Yang, H.; Xiao, L.; Lai, B.; Zhang, M.; Ni, J.; Luo, Z.; Zhang, Z.; Huang, Y. Nuciferine relaxes rat mesenteric arteries through endothelium-dependent and -independent mechanisms. *Br. J. Pharmacol.* **2015**, *172*, 5609−5618.

(20) Xu, Y.; Bao, S.; Tian, W.; Wen, C.; Lin, C. Tissue distribution model and pharmacokinetics of nuciferine based on UPLC-MS/MS and BP-ANN. *Int. J. Clin. Exp. Med.* **2015**, *8*, 17612.

(21) Fan, Y.; et al. Comprehensive Metabolomic Characterization of Coronary Artery Diseases. *J. Am. College Cardiol.* **2016**, *68*, 1281−1293.

(22) Lin, X.; Zhang, Y.; Liu, W.; Dong, J.; Lu, J.; Di, Q.; Shi, J. Granulocyte-macrophage colony-stimulating factor-transfected bone marrow stromal cells for the treatment of ischemic stroke. *Neural Regener. Res.* **2012**, *07*, 1220−1227.

(23) Shah, F. A.; Gim, S. A.; Kim, M. O.; Koh, P. O. Proteomic identification of proteins differentially expressed in response to resveratrol treatment in middle cerebral artery occlusion stroke model. *J. Vet. Med. Sci.* **2014**, *76*, 1367−74.

(24) Jeon; Seong-Jun; Gim; Sang-Ah; Koh; Phil-Ok; Shah; Fawad-Ali; Kim; Myeong-Ok. Identification of proteins regulated by curcumin in cerebral ischemia. *J. Surg. Res.: Clin. Lab. Invest.* **2016**, *201*, 141−148.

(25) Shah, F. A.; Kury, L. A.; Li, T.; Zeb, A.; Li, S.; et al. Polydatin Attenuates Neuronal Loss via Reducing Neuroinflammation and Oxidative Stress in Rat MCAO Models. *Front. Pharmacol.* **2019**, *10*, 663.

(26) Field, K. J.; White, W. J.; Lang, C. M. Anaesthetic effects of chloral hydrate, pentobarbitone and urethane in adult male rats. *Lab. Animals* **1993**, *27*, 258.

(27) Jiang, W.; Zhang, S.; Zhu, H.; Hou, J.; Tian, J. Cornin ameliorates cerebral infarction in rats by antioxidant action and stabilization of mitochondrial function. *Phytother. Res Ptr.* **2010**, *24*, 547−552.

https://dx.doi.org/10.1021/acsomega.0c05388
ACS Omega 2020, 5, 33433−33444

(28) Shlomi, T.; Cabili, M. N.; Ruppin, E. Predicting metabolic biomarkers of humaninborn errors of metabolism. *Mol. Syst. Biol.* **2009**, *5*, 263.
(29) Shi, J.; Zhou, J.; Ma, H.; Guo, H.; Ni, Z.; et al. An in vitro metabolomics approach to identify hepatotoxicity biomarkers in human L02 liver cells treated with pekinenal, a natural compound. *Bioanal. Chem.* **2016**, *408*, 1413−1424.
(30) Xiong, Z.; Yang, J.; Huang, Y.; Zhang, K.; Bo, Y.; Lu, X.; et al. Serum metabonomics study of anti-depressive effect of Xiao-Chai-Hu-Tang on rat model of chronic unpredictable mild stress. *J. Chromatogr. B. Anal. Technol. Biomed. Life* **2016**, *1029-1030*, 28−35.
(31) Zhou, C.; Jia, H. M.; Liu, Y. T.; Yu, M.; Chang, X.; Ba, Y. M.; Zou, Z. M. Metabolism of glycerophospholipid, bile acid and retinol is correlated with the early outcomes of autoimmune hepatitis. *Mol. Biosyst.* **2016**, *12*, 1574−1585.
(32) Tian, J.-S.; Liu, S.-B.; He, X.-Y.; Xiang, H.; Chen, J.-L.; Gao, Y.; Zhou, Y.-Z.; Qin, X.-M. Metabolomics studies on corticosterone-induced PC12 cells: A strategy for evaluating an in vitro depression model and revealing the metabolic regulation mechanism. *Neurotoxicol. Teratol.* **2018**, *69*, 27−38.
(33) Bahr Hosseini, M.; Hou, J.; Bikson, M.; Iacoboni, M.; Saver, J. L. Central Nervous System Electrical Stimulation for Neuroprotection in Acute Cerebral Ischemia: Meta-Analysis of Preclinical Studies. *Stroke* **2019**, *50*, 2892−2901.
(34) Wang, F.; Ji, S.; Wang, M.; Liu, L.; Ji, B.; et al. HMGB1 promoted P-glycoprotein at the blood-brain barrier in MCAO rats via TLR4/NF-κB signaling pathway. *Eur. J. Pharmacol.* **2020**, *880*, No. 173189.
(35) Feigin, V. L.; Forouzanfar, M. H.; Krishnamurthi, R.; Mensah, G. A.; Murray, C.; et al. Global and regional burden of stroke during 1990-2010: findings from the Global Burden of Disease Study 2010. *Lancet* **2014**, *383*, 245−255.
(36) Longa, E. Z.; Weinstein, P. R.; Carlson, S.; Cummins, R. Reversible middle cerebral artery occlusion without craniectomy in rats. *Stroke* **1989**, *20*, No. 84.
(37) Tang, H.; Gamdzyk, M.; Huang, L.; Gao, L.; Zhang, J. H.; et al. Delayed recanalization after MCAO ameliorates ischemic stroke by inhibiting apoptosis via HGF/c-Met/STAT3/Bcl-2 pathway in rats. *Exp. Neurol.* **2020**, *330*, No. 113359.
(38) Huang, J.; Upadhyay, U. M.; Tamargo, R. J. Inflammation in stroke and focal cerebral ischemia. *Surg. Neurol.* **2006**, *66*, 232−245.
(39) Jin, G.; Arai, K.; Murata, Y.; Wang, S.; Stins, M. F.; Lo, E. H.; Van Leyen, K. Protecting against cerebrovascular injury: contributions of 12/15-lipoxygenase to edema formation after transient focal ischemia. *Stroke* **2008**, *39*, 2538.
(40) Schwab, J. M.; Nan, C.; Arita, M.; Serhan, C. N. Resolvin E1 and protectin D1 activate inflammation-resolution programmes. *Nature* **2007**, *447*, 869−874.
(41) Neubauer, H. A.; Pitson, S. M. Roles, regulation and inhibitors of sphingosine kinase 2. *Febs J.* **2013**, *280*, 5317−5336.
(42) Huwiler, A.; Pfeilschifter, J. New players on the center stage: sphingosine 1-phosphate and its receptors as drug targets. *Biochem. Pharmacol.* **2008**, *75*, 1893−1900.
(43) Yin, P.; Wan, D.; Zhao, C.; Chen, J.; Zhao, X.; Wang, W.; Lu, X.; Yang, S.; Gu, J.; Xu, G. A metabonomic study of hepatitis B-induced liver cirrhosis and hepatocellular carcinoma by using RP-LC and HILIC coupled with mass spectrometry. *Mol. Biosyst.* **2009**, *5*, 868−876.
(44) Bryan, L.; Kordula, T.; Spiegel, S.; Milstien, S.; Milstien, S. Regulation and functions of sphingosine kinases in the brain. *Biochim. Biophys. Acta* **2008**, *1781*, 459−466.
(45) Blondeau, N.; Lai, Y.; Tyndall, S.; et al. Distribution of sphingosine kinase activity and mRNA in rodent brain. *J Neurochem.* **2007**, *103*, 509−517.
(46) Wacker, B. K.; Park, T. S.; Gidday, J. M. Hypoxic preconditioning-induced cerebral ischemic tolerance: role of microvascular sphingosine kinase 2. *Stroke* **2009**, *40*, 3342.
(47) Pfeilschifter, W.; Czech-Zechmeister, B. E.; Sujak, M.; Mirceska, A.; Koch, A.; Rami, A.; Steinmetz, H.; Foerch, C.; Huwiler, A.; Pfeilschifter, J. Activation of sphingosine kinase 2 is an endogenous protective mechanism in cerebral ischemia. *Biochem. Biophys. Res. Commun.* **2011**, *413*, 212−217.
(48) Kraig, R. P.; Pulsinelli, W. A.; Plum, F. Hydrogen ion buffering during complete brain ischemia. *Brain Research.* **1985**, *342*, 281−290.
(49) Cloonan, L.; Fitzpatrick, K. M.; Kanakis, A. S.; et al. Metabolic determinants of white matter hyperintensity burden in patients with ischemic stroke. *Atherosclerosis.* **2015**, *240*, 149−153.
(50) Meloni, B. P. Pathophysiology and Neuroprotective Strategies in Hypoxic-Ischemic Brain Injury and Stroke. *Brain.* **2017**, *7*, 110.
(51) Boatright, J. H.; Nickerson, J. M.; Moring, A. G.; Pardue, M. T. Bile acids in treatment of ocular disease. *J Ocul Biol Dis Inf.* **2009**, *2*, 149−159.
(52) Kyle, R.; Gronbeck; Rodrigues, Cecilia M. P.; Mahmoudi, Javad.; Bershad, Eric M. Application of Tauroursodeoxycholic Acid for Treatment of Neurological and Non-neurological Diseases: Is There a Potential for Treating Traumatic Brain Injury? *Neurocritical Care.* **2016**, *25*, 153−166.
(53) Amaral, J. D.; Viana, R. J.; Ramalho, R. M.; Steer, C. J.; Rodrigues, C. M. Bile acids: regulation of apoptosis by ursodeoxycholic acid. *J Lipid Res.* **2009**, *50*, 1721−1734.
(54) Elmore, S. Apoptosis: a review of programmed cell death. *Toxicol Pathol.* **2007**, *35*, 495−516.
(55) Rodrigues, C. M. P.; et al. Neuroprotection by a Bile Acid in an Acute Stroke Model in the Rat. *J. Cereb. Blood Flow\ Metab.* **2015**, 463−471.

https://dx.doi.org/10.1021/acsomega.0c05388
ACS Omega 2020, 5, 33433−33444